Fiber-optic sensor based on Michelson interferometers for distributed disturbance detection

Li Qin[1,2], Wang Hongbo[3], Li Lijing[1], Liang Sheng[4], Zhong Xiang[1]

(1. School of Instrument Science and Opto-electronics Engineering, Beihang University, Beijing 100191, China;
2. The Third Research Institute of China Electronics Technology Group Corporation, Beijing 100015, China;
3. Institute of Shanghai Aerospace Control Technology, China Aerospace Science and Technology Corporation, Shanghai 200233, China; 4. Key Laboratory of Education Ministry on Luminescence and Optical Information Technology, Department of Physics, School of Science, Beijing Jiaotong University, Beijing 100044, China)

Abstract: A fiber-optic distributed sensor based on Michelson interferometers for detecting the time-varying disturbance was presented in the paper. The proposed sensor is constituted of two Michelson interferometers with an optical fiber delay loop. The disturbance causes a phase modulation which is detected by the proposed sensor and converted to the location information. The interference signals received by the photo detectors through capacitive coupling separated directly to eliminate the DC component are preprocessed by the peak-to-peak value calculation method. The phase information of the preprocessed signals is acquired by the Hilbert transform, phase unwrapping and the corresponding trigonometric equations calculation. The frequency spectrum analysis and the mathematical operations are then conducted to locate the disturbance. Experimental results obtained with a 20 km long sensing fiber are discussed in the paper. The proposed distributed disturbance sensor has the significant advantages of capability of real time sensing, insensitive to the polarization state and low cost.

Key words: fiber-optic distributed disturbance sensor; interferometric sensors; Michelson interferometer
CLC number: TP212 Document code: A Article ID: 1007-2276(2015)01-0205-05

基于 Michelson 干涉仪的光纤分布式扰动传感器

李 勤[1,2],王洪波[3],李立京[1],梁 生[4],钟 翔[1]

(1. 北京航空航天大学 仪器科学与光电工程学院,北京 100191;
2. 中国电子科技集团公司第三研究所,北京 100015;
3. 中国航天科技集团公司 上海航天控制技术研究所,上海 200233;
4. 北京交通大学 理学院 物理系 发光与光信息技术教育部重点实验室,北京 100044)

摘 要: 提出并研究了基于 Michelson 干涉仪的应用于检测时变扰动的光纤分布式传感器。所提出的光纤传感器由两个 Michelson 干涉仪和一个光纤延迟环组成。扰动作用在传感光纤上,引起传输光波

收稿日期: 2014-05-17; **修订日期:** 2014-06-18
基金项目: 国家自然科学基金(61205074)
作者简介: 李勤(1983-),工程师,博士,主要从事光纤传感技术、测控技术与方法、智能仪器与虚拟仪器技术等方面的研究。
Email:liqin_buaa@163.com

相位的调制作用，可以通过该传感器进行检测并得到扰动的位置信息。通过光电探测器对干涉信号进行接收。对接收到的信号进行隔直，并通过求取峰峰值的方法对隔直后的信号进行预处理。通过希尔伯特变换、相位去包裹和三角函数运算可以提取出预处理信号中包含的相位信息。最后，通过频谱分析和相应的数学运算可以实现扰动的定位。在 20 km 的监测距离内通过实验验证了传感器的可行性。所提出的光纤传感器具有实时性好、抗偏振性、低成本的独特优势。

关键词：光纤分布式扰动传感器； 干涉型传感器； Michelson 干涉仪

0 Introduction

Fiber-optic distributed sensors can measure variables continuously along the whole length of the sensing fiber[1-2]. Compared with conventional security system, interferometer based fiber-optic distributed disturbance sensor (FDDS) has high sensitivity and is immune to electromagnetic interference and chemical corrosion. So, there has been an intense interest in development of FDDS and the sensor is extensively used for monitoring and securing national borders, oil and gas pipelines, communication links and structural health. The configurations of current interferometer based FDDS include Mach-Zehnder and Mach-Zehnder interferometers[3-4], Sagnac and Mach-Zehnder interferomters[5-6], Sagnac and Michelson interferometers[7-8], Sagnac and Sagnac interferometers[9-10], single Sagnac interferometer[11], and Sagnac interferometer with dual-wavelength[12] or working in two modes[13] and differentiating ring[14].

For FDDS based on Sagnac interferometer merged with Mach-Zehnder or Michelson interferometer, there are several disadvantages. For instance, the preferred light source for the Sagnac interferometer should be broadband. On the contrary, the Mach-Zehnder interferometer requires a light source with a long coherence length. For other interferometers based FDDS mentioned above, the problem of polarization induced fading (PIF)[15] will cause variation of the visibility and the reduction of the signal-to-noise ratio (SNR), which results in the increase of the location error and even failure of locating the disturbance.

This paper presents a distributed sensor based on Michelson interferometers. The Faraday rotator mirrors (FRMs) are fused at the end of the fiber to eliminate the PIF[16-17]. The operating principles of the sensor and the algorithm for calculating the disturbance position is analyzed and described. Furthermore, the feasibility and performance of the proposed sensor is experimentally investigated.

1 Theory

The sensor consists of two Michelson interferometers and each interferometer includes a sensing arm and a reference arm. The disturbance effecting on the fiber induces a phase modulation. The proposed Michelson interferometer based FDDS is shown in Fig.1. The light from a laser source is divided into two paths with the same power by the coupler C_1. Then the light launches into the two

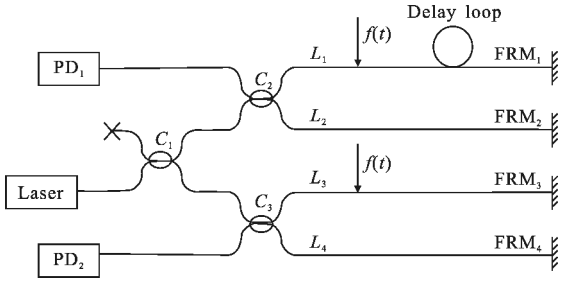

Fig.1 Schematic illustruation of the proposed sensor

interferometers formed by the two couples, a time delay loop and four Faraday rotator mirrors (FRMs). The FRMs located at the end of the optical fiber arms to eliminate the polarization induced fading. The delay loop is near the FRM_1, which is also at the end of the sensing arm L_1. The light waves propagating along the

fiber arms are reflected by the FRMs and finally interfere in C_2 and C_3 respectively. In the practical applications, reference arms are isolated from the disturbances and the sensing arms are located in the optical fiber cable.

When the disturbance occurs, the length and the reflective index of the fiber will change and induce the phase modulation. The interference lights are the superposed lightwaves that propagating towards the coupler and toward the FRM. In accordance with coherent lightwave theory, the interference signals can be derived as:

$$I_1=\frac{1}{4}I_0+\frac{1}{8}I_0\{\cos\left[f\left(t-\frac{nz}{c}\right)+\frac{4\pi nD}{\lambda}+\varphi_0\right]+\cos\left[f\left(t-\frac{2(L+D)-z}{c}n\right)+\frac{4\pi nD}{\lambda}+\varphi_0\right]\} \quad (1)$$

$$I_2=\frac{1}{4}I_0+\frac{1}{8}I_0\{\cos\left[f\left(t-\frac{nz}{c}\right)+\varphi_0'\right]+\cos\left[f\left(t-\frac{n(2L-z)}{c}\right)+\varphi_0'\right]\} \quad (2)$$

where I_0 is the optical power of the laser, φ_0 and φ_0' are the initial phases induced by the length differences of the arms, L is the length of the optical fiber arms except L_1, D is the length of the delay loop, z is the distance of the disturbance from C_2, $f(t)$ is the phase modulation caused by the disturbance, c is the speed of light in a vacuum, and n is the reflective index of the fiber.

The direct current (DC) terms of the signals are filtered in the circuit. Then I_0 is computed through peak-to-peak value calculation method. The signals can be expressed as:

$$I_3(t)=\cos\left[f\left(t-\frac{nz}{c}\right)+\frac{4\pi nD}{\lambda}+\varphi_0\right]+\cos\left[f\left(t-\frac{2(L+D)-z}{c}n\right)+\frac{4\pi nD}{\lambda}+\varphi_0\right] \quad (3)$$

$$I_4(t)=\cos\left[f\left(t-\frac{nz}{c}\right)+\varphi_0'\right]+\cos\left[f\left(t-\frac{n(2L-z)}{c}\right)+\varphi_0'\right] \quad (4)$$

Hilbert transform [18-19] are conducted to Eq.(3) and Eq.(4), we can obtain:

$$I_5(t)=\sin\left[f\left(t-\frac{nz}{c}\right)+\frac{4\pi nD}{\lambda}+\varphi_0\right]+\sin\left[f\left(t-\frac{2(L+D)-z}{c}n\right)+\frac{4\pi nD}{\lambda}+\varphi_0\right] \quad (5)$$

$$I_6(t)=\sin\left[f\left(t-\frac{nz}{c}\right)+\varphi_0'\right]\sin\left[f\left(t-\frac{n(2L-z)}{c}\right)+\varphi_0'\right] \quad (6)$$

Eq.(3) divided by (5) and Eq.(4) divided by (6), which can be given by:

$$I_7(t)=\tan\left[\frac{f\left(t-\frac{nz}{c}\right)+f\left(t-\frac{2(L+D)-z}{c}n\right)}{2}+\frac{4\pi nD}{\lambda}+\varphi_0\right] \quad (7)$$

$$I_8(t)=\tan\left[\frac{f\left(t-\frac{nz}{c}\right)+f\left(t-\frac{2(L+D)-z}{c}n\right)}{2}+\varphi_0\right] \quad (8)$$

Then it can be derived as:

$$I_9(t)=\tan\left[f\left(t-\frac{nz}{c}\right)+f\left(t-\frac{2(L+D)-z}{c}n\right)+\frac{8\pi nD}{\lambda}+2\varphi_0\right] \quad (9)$$

$$I_{10}(t)=\tan\left[f\left(t-\frac{2L-z}{c}n\right)+f\left(t-\frac{nz}{c}\right)+2\varphi_0\right] \quad (10)$$

Here phase unwrapping algorithm [20] of tangent function is applied to Eq.(9) and (10), which can be deduced:

$$I_{11}(t)=f\left(t-\frac{nz}{c}\right)+f\left(t-\frac{2(L+D)-z}{c}n\right)+\frac{8\pi nD}{\lambda}+2\varphi_0 \quad (11)$$

$$I_{12}(t)=f\left(t-\frac{2L-z}{c}n\right)+f\left(t-\frac{nz}{c}\right)+2\varphi_0' \quad (12)$$

Since φ_0 and φ_0' are the slowly drifting phases, which can be filtered, we can obtain:

$$I_{13}(t)=f\left(t-\frac{nz}{c}\right)+f\left(t-\frac{2(L+D)-z}{c}n\right) \quad (13)$$

$$I_{14}(t)=f\left(t-\frac{2L-z}{c}n\right)+f\left(t-\frac{nz}{c}\right) \quad (14)$$

In case that the disturbance induced phase modulation on the fiber is given by:

$$f(t)=A\cos(\omega t+\varphi) \quad (15)$$

where A, ω and φ are the amplitude, angular frequency and initial phase of the phase modulation, respectively.

From Eq. (13) and (14), the signals can be expressed as:

$$I_{13}(t)=A\cos\left[\omega\left(t-\frac{nz}{c}\right)+\varphi\right]+A\cos\left[\omega\left(t-n\frac{2(L+D)-z}{c}\right)+\varphi\right] \quad (16)$$

$$I_{14}(t)=A\cos\left[\omega\left(t-\frac{nz}{c}\right)+\varphi\right]+A\cos\left[\omega\left(t-\frac{n(2L-z)}{c}\right)+\varphi\right] \quad (17)$$

Then it can be deduced as:

$$I_{13}(t)=2A\cos\left[\omega\left(\frac{n(L+D-z)}{c}\right)\right]\cos\left[\omega\left(t-\frac{n(L+D)}{c}\right)+\varphi\right] \quad (18)$$

$$I_{14}(t)=2A\cos\left[\omega\left(\frac{n(L-z)}{c}\right)\right]\cos\left[\omega\left(t-\frac{nL}{c}\right)+\varphi\right] \quad (19)$$

Frequency spectrum analysis is conducted to Eqs.

(18) and (19), which can be obtained:

$$z=L-\frac{2D_2-KD_1}{2(K-1)} \tag{20}$$

$$z=L-\frac{2D_2-KD_1}{2(K-1)} \tag{21}$$

Eq. (20) divided by (21) makes the result:

$$z=L-\frac{2D_2-KD_1}{2(K-1)} \tag{22}$$

So, the location of the disturbance z can be calculated by Eq. (22). If the values inside the trigonometric functions approximates to zero, Eq.(22) can be derived by the equivalent infinitesimal substitution method:

$$z=L-\frac{2D_2-KD_1}{2(K-1)} \tag{23}$$

Then the location of the disturbance is as follows:

$$z=L-\frac{2D_2-KD_1}{2(K-1)} \tag{24}$$

where

$$z=L-\frac{2D_2-KD_1}{2(K-1)} \tag{25}$$

2 Experiment and discussion

To verify the feasibility of the proposed sensor, the setup of the prototype system is built and shown in Fig.1. In general, the setup includes a laser source, three couplers, several sensing fiber loop, four FRM, two photo detectors (PDs), a data acquisition card (DAQ) and a computer. The central wavelength of the laser is about 1 550.0 nm, the maximum output power is about 25 mW and the linewidth is about 5 kHz. The monitored length of the sensing fibers and the reference fibers are 20 km. The length of the delay loop is 10 km. The sampling frequency of the DAQ is 2 MHz. In order to test the distributed sensing performance, the PZTs are driven by a function generator with two channels to produce the 1 kHz cosinusoidal disturbances to the sensing fiber arms (L_2 and L_3) at five positions.

The detected signal induced by the perturbation at the position z =10 km is shown in Fig.2, from which we can see that the proposed sensor is able to detect the disturbance. (A) and (B) are the signals from the two Michelson interferometers respectively. At first, the signals from the PDs are preprocessed to obtain I_3 and I_4. Then the mathematical operations and frequency spectrum analysis are performed to obtain the amplitude spectrum of the signals. Then the position of the disturbance can be calculated from Eq. (22). The measured and actual location of the disturbance is presented in Fig.3, from which it is clear that the maximal error is 350 m and the average error is 230 m. The location performance of the sensor can be improved with higher precision of the frequency spectrum analysis.

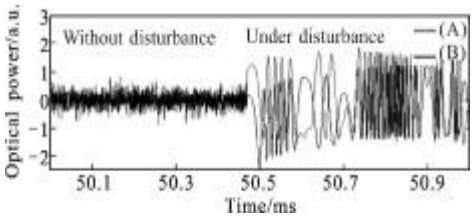

Fig.2 Detected signal induced by the perturbation at the position z=10 km

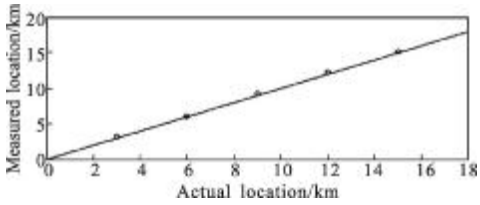

Fig.3 Measured versus actual location of the disturbance

3 Conclusion

The Michelson interferometers based fiber-optic sensor for sensing and locating the distributed disturbance is demonstrated in the paper. Compared with other interferometer based FDDS, the sensor is able to eliminate the PIF by employing the FRMs. By mathematical operations and frequency spectrum analysis, the location of the disturbance can be calculated. The experimental results confirm the design and the theoretical analysis. The proposed sensor has the advantages of strong antijamming ability, real-time and high sensitivity. Future investigation will be focused on developing the sensor for field tests in the

practical applications.

References:

[1] Udd E. Sagnac distributed sensor concepts [C]//SPIE, 1991, 1586: 46-52.

[2] Xu Wenyuan, Zhang Chunxi, Liang Sheng, et al. Fiber-optic distributed sensor based on a Sagnac interferometer with a time delay loop for detecting time-varying disturbance [J]. Microwave and Optical Technology Letters, 2009, 51(11): 2564-2567.

[3] Zhang Chunxi, Li Qin, Liang Sheng, et al. Location algorithm for multi-disturbances in fiber-optic distributed disturbance sensor using a Mach-Zehnder interferometer [C]// International Conference on Optical Communications and Networks, 2010: 103-107.

[4] Ouyang Dian, Zhou Jinfeng. Research on polarization state in fiber sensor based on Mach-Zehnder interferometer [J]. Infrared and Laser Engineering, 2008, 37(Z): 94-97. (in Chinese)

[5] Chtcherbakov A A, Swart P L, Spammer S J, et al. A modified Sagnac/Mach-Zehnder interferometer for distributed disturbance sensing[C]//SPIE, 1998, 3489: 60-64.

[6] Chtcherbakov A A, Swart P L, Spammer S J. Mach-Zehnder and modified Sagnac-distributed fiber-optic impact sensor [J]. Applied Optics, 1998, 37: 3432-3437.

[7] Kondrat M, Szustakowski M, Palka N, et al. A Sagnac-Michelson fibre optic interferometer: signal processing for disturbance localization [J]. Opto-Electronics Review, 2007, 15: 127-132.

[8] Qian Ruihai, Meng Yingjun. Application for micro-vibration measurement with a semiconductor laser interferometer [J]. Infrared and Laser Engineering, 1999, 28(2): 37-39. (in Chinese)

[9] McAulay A D, Wang J. A Sagnac interferometer sensor system for intrusion detection and localization [C]//SPIE, 2004, 5435: 114-119.

[10] Fang X J. A variable-loop Sagnac interferometer for distributed impact sensing [J]. IEEE Journal of Lightwave Technology, 1996, 14: 2250-2254.

[11] Hoffman P R, Kuzyk M G. Position determination of an acoustic burst along a Sagnac interferometer [J]. IEEE Journal of Lightwave Technology, 2004, 22: 494-498.

[12] Russell S J, Brady K R, Dakin J P. Real-time location of multiple time-varying strain disturbances, acting over a 40-km fiber section, using a novel dual-Sagnac interferometer [J]. Journal of Lightwave Technology, 2001, 19: 205-213.

[13] Fang X J. Fiber-optic distributed sensing by a two-loop Sagnac interferometer[J]. Optics Letters, 1996, 21: 444-446.

[14] Spammer S J, Swart P L, Booysen A. Interferometric distributed optical-fiber sensor [J]. Applied Optics, 1996, 35(22): 4522-4525.

[15] Kersey A D, Marrone M J, Dandridge A. Observation of input-polarization-induced phase noise interferometric fiber-optic sensors [J]. Optics Letters, 1988, 13: 847-849.

[16] Ferreira L A, Santos J L, Farahi F. Polarization-induced noise in a fiber-optic Michelson interferometer with Faraday rotator mirror elements [J]. Applied Optics, 1995, 34: 6399-6402.

[17] Wu Yuefeng, Li Fang, Zhang Wentao, et al. Polarization-induced phase noise in fiber-optic Michelson interferometer with Faraday rotator mirrors[C]//SPIE, 2008, 7134: 1-7.

[18] Lv Jie, Wang Ming, Huan Hai, et al. Fringe analysis with Hilbert transform and its application in the measurement of aspheric mirror[J]. Acta Optica Sinica, 2005, 25(6): 781-785. (in Chinese)

[19] He Junfeng, Liu Wenqing, Zhang Yunjun, et al. New method of lidar ceilometer backscatter signal processing based on Hilbert-Huang transform [J]. Infrared and Laser Engineering, 2012, 41(2): 397-403. (in Chinese)

[20] Rivera M, Marroquin J L. Half-quadratic cost functions for phase unwrapping[J]. Optics Letters, 2004, 29: 504-506.